J|A|C|S
COMMUNICATIONS

Published on Web 11/21/2006

Supra-Assembly of Siliceous Vesicles

Hongning Wang,† Xufeng Zhou,† Meihua Yu,† Yunhua Wang,† Lu Han,† Jun Zhang,† Pei Yuan,† Graeme Auchterlonie,‡ Jin Zou,‡ and Chengzhong Yu*,†

Department of Chemistry and Shanghai Key Laboratory of Molecular Catalysis and Innovative Materials, Fudan University, Shanghai 200433, P. R. China, and School of Engineering and Centre for Microscopy and Microanalysis, The University of Queensland, QLD 4072, Australia

Received September 17, 2006; E-mail: czyu@fudan.edu.cn

Besides their importance in global cycling of carbon and silicon,[1] diatoms are fascinating because of their species-specific cell walls (so-called frustules). The frustules are composed of amorphous silica and a small proportion of associated organic macromolecules, usually patterned in beautiful and symmetrical architectures from nano- to macroscale.[2] For example, the deposited silica in *D. brightwellii*[3] and *N. salinarum*[4] exhibits a hexagonal column pattern, in which each column is usually surrounded by six others. It is believed that the frustules are produced through a biomineralization process in vivo, which involves polymerization and deposition of silicic acid controlled by organic species.

The porosity, pore size, and pore architecture of frustules are important because their mechanical[5,6] and optical properties[7] depend strongly upon their structural characteristics. The origin of ordered macropores or very large mesopores found in some diatoms[2,4] have puzzled scientists for centuries, and their formation mechanisms are still under investigation.[8−11] Although similar porous materials have been successfully synthesized by means of emulsion,[12] microemulsion,[13] or colloidal sphere templating methods,[14] these techniques are either chemical based that need a significant amount of organic additives or hard-template based to produce large pores. However, natural frustules produced by the biomineralization process do not need a large amount of organic solvents or hard templates to produce large pores. As a consequence, the synthesis of artificial materials that mimics frustules is a current challenge, which can provide a different insight into the formation mechanism of frustules and, in turn, lead to significant applications in silica chemistry, materials science, and nanotechnology.

Here, we report a new approach to produce macroporous (∼110 nm in diameter) ordered siliceous foams (MOSF) in the presence of poly(ethylene oxide)-poly(propylene oxide)-poly(ethylene oxide) ($EO_{20}PO_{70}EO_{20}$, denoted P123, BASF) copolymers. The synthesis was carried out at 35 °C in pH = 5.0 buffer solutions in the absence of organic cosolvent (Supporting Information), similar to the biosilica formation process in the slightly acidic environment in silica deposition vesicles (SDV) in diatoms.[15]

Figure 1 shows scanning electron microscopy (SEM) images of MOSF. Large scale uniform hexagonally arrayed columns can be observed when viewed from the top (Figure 1a), resembling the hexagonal column pattern in some diatoms.[3,4] The pore size is estimated to be ∼100 nm. Figure 1b is an SEM image from a tilted sample and shows clearly two columnar layers. Extensive SEM investigation showed that the majority of MOSF possess up to three columnar layers. It is of interest to note that some spheres are embedded in the ordered hexagonal array (as shown in Figure 1b).

Figure 1c is a typical transmission electron microscopy (TEM) image of MOSF and shows complicated but regular patterns.

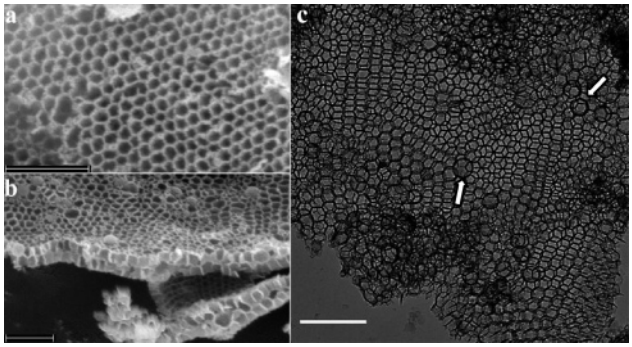

Figure 1. SEM (a, b) and TEM (c) images of MOSF: (a) viewed from the top and (b) viewed inclined. Some spheres embedded in the ordered foams are observed in image b and further confirmed as unilamellar vesicles as marked by arrows shown in image c. Scale bar is 500 nm in all images.

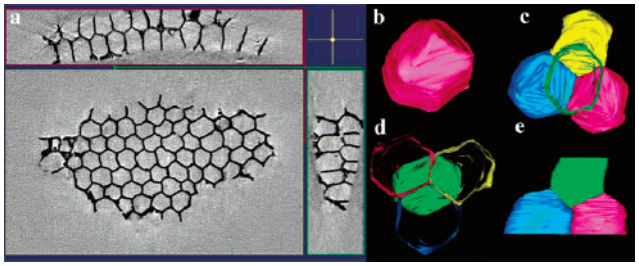

Figure 2. ET image (a) and the reconstructed structure (b−e) of MOSF showing (b) one cell and, in images c, d, and e, four neighbored cells viewed from top, bottom, and side, respectively.

Interestingly, the spheres found in SEM have been confirmed as unilamellar vesicles in the TEM image (marked by arrows). The size distribution of vesicles is relatively uniform with an average diameter of 125 ± 10 nm and the mean wall thickness of ∼6 nm.

To solve the genuine 3D suprastructure, electron tomography (ET) was used to determine the detailed porous structure of MOSF. Two series of TEM images were taken when a sample was tilted from +60 to −60° at a step of 1° in two perpendicular axes. Using the IMOD program[16] the tomograms along the electron beam can be created. Figure 2a shows the tomograms of the sample at a selected position (yellow cross) viewed from three directions. It is obvious that the sample has a bilayer structure from two perpendicular side views. Each cell is a hexagonal prism with one open end and the other end being closed and linked with three adjacent cells from the other layer. By tracing the contours of four neighboring cells, the precise structure of the cells can be reconstructed (shown in Figure 2).

Figure 2b exhibits one cell with detailed information of the close end (bottom) which is composed of three identical rhombuses with a common vertex and each of them is connected with two of six

† Fudan University.
‡ The University of Queensland.

10.1021/ja066707o CCC: $33.50

Scheme 1. The Proposed Formation Mechanism that Spans from the Atomic to the Macroscopic Scale[a]

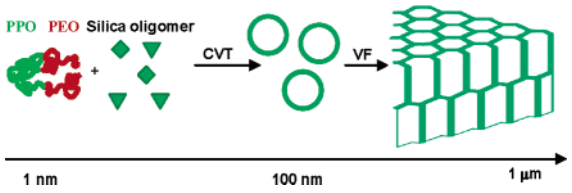

[a] The cooperative vesicle templating (CVT) of block copolymers and siliceous species gives rise to unilamellar vesicles ~100 nm in diameter. Further vesicle fusion (VF) of unilamellar vesicles with uniform sizes results in MOSF with well-defined honeycomb structure at the micrometer-scale.

side facets of the hexagonal prism. When viewed from the top, these six side facets become hexagonally arrayed struts in the projections observed in conventional TEM images (Figure 1c). The packing of the suprastructure in MOSF is revealed by the model of four neighbored cells shown in Figure 2c, d, and e (top, bottom, and side view, respectively). The bottom of the cell (the green one) in one layer is filled in the interspace created by three other closely packed cells (the yellow, red, and blue ones) located at the other layer. The extension of this basic structural model in two dimensions can construct a uniform MOSF, as observed by SEM and TEM. Such a model is identical to a perfect structure of a three-dimensional honeycomb found in honeybees, which is believed to be one of the most efficient ways to utilize space in nature.[17,18]

It should be noted that the MOSF material has been synthesized at a high concentration of Na_2SO_4 (0.4 M). When the concentration of Na_2SO_4 is adjusted between 0.1 and 0.4 M (keeping the other reaction conditions identical), a vesicle → tightly aggregated vesicle → MOSF structural transition has been observed. In another series of experiments, the structure evolution as a function of time was studied during the formation of MOSF. Cryo TEM observations show the existence of hollow spheres in solution ~1 h after the addition of a silica source, while the formation of the macroporous structure is commenced after ~3 h as evidenced from the direct SEM observations. Further increasing the reaction time and the additional hydrothermal treatment may favor the formation of ordered MOSF materials as shown in Figure 1.

On the basis of the above experimental observations, a formation mechanism of MOSF that spans from the atomic scale to the macroscopic scale can be proposed and is shown in Scheme 1. Unlike the direct vesicle templating approach of siliceous vesicles on preformed organic vesicles,[19] the formation of unilamellar composite vesicles is suggested to follow a cooperative vesicle templating process between macromolecules and siliceous species because only a multilamellar vesicular phase was observed in this block copolymer solution.[20] At high ionic strength (0.4 M Na_2SO_4), it is observed that gelation occurs in the entire reaction vessel only ~15 min after the addition of silica source, indicating that the silica species are only partially condensed. The fusion of soft unilamellar composite vesicles[21] with relatively uniform size finally results in MOSF material with well ordered and defined honeycomb structures at the macroscale, which is energetically beneficial.[17,18] The pore opening in MOSF material is most likely attributed to the capillary force during the drying process. Our results also suggest that the hydrothermal treatment is helpful to open the pores in MOSF materials. The uniform pore-size distribution curve of MOSF centered at ~110 nm suggests that the size distribution of composite vesicles may become narrower either at increased ionic strength or during the vesicle fusion process.

It is noted that the fusion of vesicles to ordered structures is a subject closely related to the Kelvin conjecture (how to fill space with bubbles) and the honeycomb conjecture (the honeycomb architecture used the least amount of material). We use the electron tomography to solve the elegant 3D hexagonal structure of MOSF; more importantly, we first show that the self-assembled inorganic−organic composite vesicles may behave just like "bubbles", which further self-assemble into 3D hexagonal suprastructures. Although organic and hybrid large compound vesicles (LCVs) have been synthesized,[21,22] the synthetic approaches involved organic cosolvents, and the structure of the LCVs is disordered. Our synthesis is carried out under mild conditions similar to the biosilica deposition environment in diatoms, and the resultant MOSF material shows a well-defined structure, which is important in understanding the formation mechanism of frustules in diatoms.

In conclusion, we have demonstrated, for the first time, that the molecular assembled compound vesicles with diameters larger than ~100 nm can be further utilized as building blocks to assemble elegant structures, similar to those of diatoms and honey-bees in nature. Our approach provides a simple and new pathway to synthesize ordered macroporous materials, which may find applications in bioimmobilization, controlled release, catalyst supports, separation materials, and thermal insulations and as low dielectric materials.

Acknowledgment. This work is supported by the NSF of China (Grants 20573021, 20421303), the State Key Research Program (Grant 2004CB217800, 2006CB0N0302), Shanghai Science Committee (Grant 05SU07098), and Shanghai Hua Yi Group.

Supporting Information Available: Synthesis details, SEM, TEM, supplementary movie (avi), N_2 sorption isotherm, and pore-size distribution curve of MOSF. This material is available free of charge via the Internet at http://pubs.acs.org.

References

(1) Field, C. B.; Behrenfeld, M. J.; Randerson, J. T.; Falkowski, P. *Science* **1998**, *281*, 237−240.
(2) Round, F.; Crawford, D.; Mann, D. *The Diatoms*; Cambridge University Press: Cambridge, U.K., 1990.
(3) Li, C. W.; Volcani, B. E. *Philos. Trans. R. Soc. London, Ser. B* **1984**, *304*, 519−528.
(4) Vrieling, E. G.; Beelen, T. P. M.; Sun, Q. Y.; Hazelaar, S.; van Santen, R. A.; Gieskes, W. W. C. *J. Mater. Chem.* **2004**, *14*, 1970−1975.
(5) Subhash, G.; Yao, S.; Bellinger, B.; Gretz, M. R. *J. Nanosci. Nanotechnol.* **2005**, *5*, 50−56.
(6) Hamm, C. E.; Merkel, R.; Springer, O.; Jurkojc, P.; Maier, C.; Prechtel, K.; Smetacek, V. *Nature* **2003**, *421*, 841−843.
(7) Fuhrmann, T.; Landwehr, S.; El Rharbi-Kucki, M.; Sumper, M. *Appl. Phys. B: Lasers Opt.* **2004**, *78*, 257−260.
(8) Sumper, M. *Angew. Chem., Int. Ed.* **2004**, *43*, 2251−2254.
(9) Vrieling, E. G.; Beelen, T. P. M.; van Santen, R. A.; Gieskes, W. W. C. *Angew. Chem., Int. Ed.* **2002**, *41*, 1543−1546.
(10) Parkinson, J.; Brechet, Y.; Gordon, R. *Biochim. Biophys. Acta* **1999**, *1452*, 89−102.
(11) Sumper, M. *Science* **2002**, *295*, 2430−2433.
(12) Imhof, A.; Pine, D. J. *Nature* **1997**, *389*, 948−951.
(13) Schmidt-Winkel, P.; Lukens, W. W.; Zhao, D. Y.; Yang, P. D.; Chmelka, B. F.; Stucky, G. D. *J. Am. Chem. Soc.* **1999**, *121*, 254−255.
(14) Velev, O. D.; Jede, T. A.; Lobo, R. F.; Lenhoff, A. M. *Nature* **1997**, *389*, 447−448.
(15) Vrieling, E. G.; Gieskes, W. W. C.; Beelen, T. P. M. *J. Phycol.* **1999**, *35*, 548−559.
(16) Kremer, J. R.; Mastronarde, D. N.; McIntosh, J. R. *J. Struct. Biol.* **1996**, *116*, 71−76.
(17) Hales, T. C. *Discrete Comput. Geom.* **2001**, *25*, 1−22.
(18) Weaire, D.; Hutzler, S. *The Physics of Foams*; Oxford University Press: Oxford, 1999.
(19) Hubert, D. H. W.; Jung, M.; Frederik, P. M.; Bomans, P. H. H.; Meuldijk, J.; German, A. L. *Adv. Mater.* **2000**, *12*, 1286−1290.
(20) Zipfel, J.; Lindner, P.; Tsianou, M.; Alexandridis, P.; Richtering, W. *Langmuir* **1999**, *15*, 2599−2602.
(21) Zhang, L. F.; Eisenberg, A. *Macromolecules* **1996**, *29*, 8805−8815.
(22) Du, J. Z.; Chen, Y. M. *Angew. Chem., Int. Ed.* **2004**, *43*, 5084−5087.

JA066707O